Infrared spectroscopy of fullerenes

1995 J. Phys.: Condens. Matter 7 6601

(http://iopscience.iop.org/0953-8984/7/33/003)

J. Phys.: Condens. Matter 7 (1995) 6601–6624. Printed in the UK

REVIEW ARTICLE

Infrared spectroscopy of fullerenes

H Kuzmany, R Winkler, and T Pichler

Universität Wien, Institut für Festkörperphysik, Strudlhofgasse 4, A-1090 Wien, and Ludwig Boltzmann Institut für Festkörperphysik Wien, Austria

Received 13 April 1995

Abstract. This review summarizes the present status of the application of IR spectroscopy to the field of fullerene science. In accord with the amount of published work the report concentrates to a large extent on the C_{60} molecule in its neutral and charged form in a crystalline environment. After a short introduction to the basic terminologies and properties of fullerenic materials a detailed description of the response of pristine C_{60} the IR radiation is given. It includes a review on the vibrational fine structure, the isotope effects, and the influence of the structural phase transitions.

For the case of the doped material the response of the free carriers and their interaction with the vibrational modes as observed in the IR spectra is reviewed, including the case of high-temperature superconductivity. Special attention is paid to the colourful behaviour of the phases AC_{60} and to the air stability of this compounds.

In the final part of the review selected examples are given for the application of IR spectroscopy to higher fullerenes and to fullerene-derived materials.

1. Introduction

Fullerenes represent a new form of carbon first discovered by Kroto and Smalley [1] in a beam of laser-evaporated graphite. In the molecules generated by this process nearly sp^2 hybridized carbon atoms are covalently bonded in a cagelike configuration. The hybridization state requires three next neighbours for each carbon which renders polyhedric molecules terminated by hexagons and pentagons. From Euler's rule which relates the number of edges of a convex polyhedron to its number of corners and planes exactly twelve pentagons and an arbitrary but even number of hexagons follow for each polyhedron. Isolated pentagons on the cage yield an increased stability. Thus, the smallest cage which allows isolated pentagons is the first stable fullerene in a series of many cages with larger size. This most stable cage consists of 60 carbons and has the highly symmetric form of a truncated icosahedron, now well known as the football-like C_{60} molecule. The point group symmetry of this molecule is I_h.

C_{60} was found to be generated in large amounts in an arc discharge process by Krätschmer *et al* [2] and was subsequently subjected to many investigations. At temperatures below 600 K the molecules form a molecular crystal with an fcc lattice which can be grown from the vapour phase to a reasonably large size and high quality [3, 4].

The impact of IR spectroscopy on the research on fullerenes is widespread. The analysis of molecular vibrations is certainly one important point which is particularly attractive for C_{60} because of the high symmetry of the molecule and the correspondingly low number of IR allowed vibrations. In the crystalline phase the symmetry of the molecule is reduced which leads to line splitting and breaking of selection rules. This gives the possibility

0953-8984/95/336601+24$19.50

to study the crystal field and the various structural phase transitions in the material by analysing the external and internal vibrational modes for either neutral or multiply charged cages. The other important field for IR spectroscopy is the analysis of electronic structures. Low-energy electronic transitions and free-carrier contributions to the response function are typical examples.

Good reviews on the state of the art in fullerene research have been published as special issues of several journals [5–7].

For the study of the fullerenes by IR spectroscopy full use is made of the rapid development of modern methods like very high resolution in energy, down to 10^{-2} cm^{-1}, or very high-power spectroscopy from synchrotron sources.

In this review we report the state of the art in IR spectroscopy of fullerenes with respect to application and results. Particular attention is paid to fullerenes in the solid phase. Since most of the work has been done so far for the C_{60} compound the greatest part of the review will be dedicated to this material. A similar paper was recently published by one of the present authors on the state of the art in Raman spectroscopy of fullerenes [8]. This article may be considered as complementary to the review presented here.

2. Fullerenes, fullerites and fullerides

2.1. The classical fullerene C_{60} in its crystalline form

The classical fullerene C_{60} has attracted a lot of attention because of its interesting structural and dynamical properties. It exhibits a structural order transition from a high-temperature state with an fcc crystal structure ($Fm3m/O_h^5$ space group) to a simple cubic structure ($Pa\bar{3}/T_h^6$ space group) [9] and a glass transition between 150 K and 80 K [10, 11]. At very low temperatures a superstructure with a doubled unit cell may develop [12]. In the high-temperature phase the C_{60} molecules are nearly free rotating which means a degeneracy of the librational modes to zero frequency or to motions which are often characterized as paralibrons. Accordingly this state is called the rotor phase. The state below the order transition is characterized by a reduced, ratchet-like motion of the molecules and is therefore called the ratchet phase. Below the glass transition the molecules are completely locked in their position and orientation.

Even though a lot of IR spectroscopy has been dedicated already to the pristine C_{60} there is still a wide interest, for example, in a high-resolution analysis of the phase transitions as will be discussed in the next section. Also, isotope clean material which allows more detailed analyses became available only recently.

2.2. Fullerides with particular attention to alkali metal compounds

The salts of the fullerenes are the fullerides. C_{60} can readily be transferred to this form by intercalation of alkali metals into the large octahedral and tetrahedral interstitials of the fcc lattice. Since the electron affinity of the C_{60} molecule is very high the s electron of the alkali metal is easily transferred to the lowest unoccupied t_{1u} orbital of the molecule which renders the latter in a negatively charged state. Depending on how many alkali metal atoms are accommodated per C_{60} a compound A_xC_{60} is obtained. Only integer values for x have been reported. For the more bulky alkali metals only the values $x = 1, 3, 4$, and 6 have been observed. For sodium $x = 2$ also exists. Since the t_{1u} derived band can accept a total of six electrons per C_{60} within a single-electron picture all alkali metal salts, except those for $x = 6$, should be metals. In practice a metallic state is only confirmed for $x = 3$

compounds. These compounds were found to be superconductors with rather high transition temperatures [13, 14, 15]. More details about the structures of the fullerides will be given in section 5.

Recently special interest was attracted by the compounds AC_{60} which exhibit another series of unusual properties. AC_{60} has a rock salt structure at high temperatures [16] but undergoes either a disproportionation to C_{60} and A_3C_{60} [17, 18] or a displacive phase transition to an orthorhombic state [19]. This state was recently even claimed to be metallic and to have polymeric character [20].

Vibrational IR spectroscopy has frequently been used to study the charged state of the molecules in these systems [21, 22, 23] but also their free-carrier response and their metallicity or superconductivity were investigated extensively [24–27].

2.3. Higher fullerenes and endohedral fullerenes

From the higher fullerenes only C_{70} has attracted attention so far, since it is the only higher fullerene which can be prepared with a similar high yield as the C_{60} molecule. This again has to do with its relative small size and its isolated pentagon character. C_{70} also undergoes several phase transitions but the lower symmetry of the molecule makes the evaluation of the experiments more difficult. This holds in particular for experiments from vibrational IR spectroscopy where the number of IR allowed vibrational modes increases rapidly not only because of the lower symmetry but also because of the larger number of atoms in the molecule. C_{70} has been investigated only to a very limited extent in the intercalated state.

Reasonable amounts of material from molecules with more than 70 carbons per cage have been prepared only to a limited extent [28, 29]. The difficulty arises not only from the low yield in the thermochemical reaction in the arc discharge but also from the increasing number of energy-equivalent isomers. Thus, isolation of individual molecular phases becomes very laborious.

Similar arguments as given above hold for the endohedral systems, where metallic or nonmetallic atoms are encapsulated into the cage [30–32]. These most interesting systems are very difficult to prepare and IR spectra exist only to a very limited extent.

In the limit of very large fullerenes which are tubelike, extended in one direction, experiments become easier. Such systems have attracted a lot of interest and are known as fullerene nanotubes. Also, IR spectroscopy becomes easier for these compounds since they approach a one-dimensional solid and are in several aspects similar to graphite.

2.4. Fulleroides and fullerene-derived structures

The final group of fullerene-type molecules are the chemically derived adduct products from the pure cage molecules. Good progress is being made in this field of fullerene research [33, 34] but vibrational spectroscopy again suffers from the complicated character of the vibrational spectra at least for the compounds with large organic adducts.

3. Vibrational selection rules for C_{60}

A good review on the selection rules for vibrational motion of the atoms in C_{60} is given in [35]. For the free and isotope clean C_{60} molecule they are rather simple. From the character table for the icosahedric point group the irreducible representations for the 174 vibrational degrees of freedom are given as

$$\Gamma_{tot} = 2A_g + 3F_{1g} + 4F_{2g} + 6G_g + 8H_g + A_u + 4F_{1u} + 5F_{2u} + 6G_u + 7H_u. \quad (1)$$

Only the F_{1u} vibrations exhibit a nonvanishing dipole moment. Thus, only four IR-active modes exist in the isotope clean and free molecule. If the molecule is accommodated in a crystal the symmetry is reduced to allow for translational invariance. Since the molecules are accommodated at lattice sites with T_h symmetry a good reference point group is T_h which allows a degeneracy only up to three. Thus, the fourfold-degenerate G- modes and the fivefold-degenerate H modes split into modes with lower degeneracy, amongst others into F_u modes. Since in T_h all F_u modes are IR active the number of IR-active modes is strongly increased. However, the dipole moment for the I_h forbidden modes is expected to be very small. The splitting of the modes goes on for the low-temperature phase where the number of C_{60} molecules per unit cell increases by a factor of four. This means a Davidov splitting for all modes and a corresponding increase of the components in the case of the originally degenerate modes. The splitting and the correlation of the modes is compiled in table 1. The last column in the table refers to a further reduction of the symmetry at very low temperatures as observed from electron microscopy. In this case the unit cell is doubled once more and the space group becomes T_h^4.

From the 24 external degrees of motional freedom in the low-temperature phase (12 *gerade* and 12 *ungerade* species) only the translational species with F_u character exhibit a dipole moment. Thus, we can expect two IR-active F_u modes for the ratchet phase and five IR-active F_u modes for the T_h^4 phase.

Table 1. Internal and external *ungerade* modes for C_{60} fullerite in the molecule and various crystal structures. Only the modes F_{1u} or F_u are IR active.

Species	Molecule I_h	Fullerite rotor phase T_h^3	Fullerite ratchet phase T_h^6	Fullerite locked phase T_h^4
Internal				
	$1A_u$	$1A_u$	$A_u + F_u$	$A_u + 4F_u$
	$4F_{1u}$	$4F_u$	$4(A_u + E_u + 3F_u)$	$8(A_u + E_u + 3F_u)$
	$5F_{2u}$	$5F_u$	$5(A_u + E_u + 3F_u)$	$10(A_u + E_u + 3F_u)$
	$6G_u$	$6(A_u + F_u)$	$6(2A_u + E_u + 4F_u)$	$12(2A_u + E_u + 4F_u)$
	$7H_u$	$7(E_u + F_u)$	$7(A_u + 2E_u + 5F_u)$	$14(A_u + 2E_u + 5F_u)$
External				
Infrared	—	—	$A_u + E_u + 2F_u$	$2A_u + 2E_u + 5F_u$
Acoustic	—	F_u	F_u	F_u

A further splitting of degenerate modes and a further activation of an IR response can be expected from an isotope effect. The concentration of 1.108% ^{13}C in natural carbon yields only 51.2% efficiency for isotope pure C_{60}. 34.5% of the material is contaminated with exactly one ^{13}C per cage. By the isotope substitution the symmetry of the cage is strongly reduced to C_s where only one-dimensional A′ and A″ modes are possible both of which are Raman and IR active. The influence of this isotope effect on the vibrational structure has been discussed several times [36, 37].

The selection rules remain similar for the intercalated phases, at least as long as the structure remains cubic. In this case we can expect to see the four F_{1u}-derived modes and some of the crystal-field-induced modes similar to the species in table 1 for the rotor phase. For the cubic phases with $x = 34$ and 6 no structural phase transition with decreasing temperature is observed. For the phase with $x = 4$ the F modes split into A + E which now represent the IR-active species. A review on the various intercalated phases and on their IR activity is given in section 5. The phase with $x = 1$ at low temperatures behaves differently

since obviously new covalent bonds are established as will be discussed in section 6.

Infrared response is also expected from electronic transitions between orbitals with different parity. Even though most of these transitions are expected in the UV–vis spectral range, for the intercalated compounds low-energy interband transitions well within the IR spectral range are also possible. In addition transitions between the three different components of the t_{1u} band are observed as well as transitions of the free-carrier system.

4. IR spectroscopy of pristine C_{60}

Originally IR spectra were used by Krätschmer *et al* as one of the techniques to identify the powder which they extracted from the soot of the discharge process as C_{60} [2]. The absorption spectrum as obtained in their experiments from a thin film is shown in figure 1 (top). The well expressed absorption peaks indicate the four IR-active F_{1u} modes at 520, 572, 1188, and 1427 cm^{-1} in very good agreement with early quantum chemical calculations on the vibrational spectrum [38]. The spectrum at the bottom of the figure is a more recent result for the IR reflectivity from a {100} face of a thick single crystal. From a fit with a Kramers–Heisenberg dielectric function (harmonic oscillators) the mode frequencies were obtained as 527, 576, 1183, and 1428 cm^{-1} in this case.

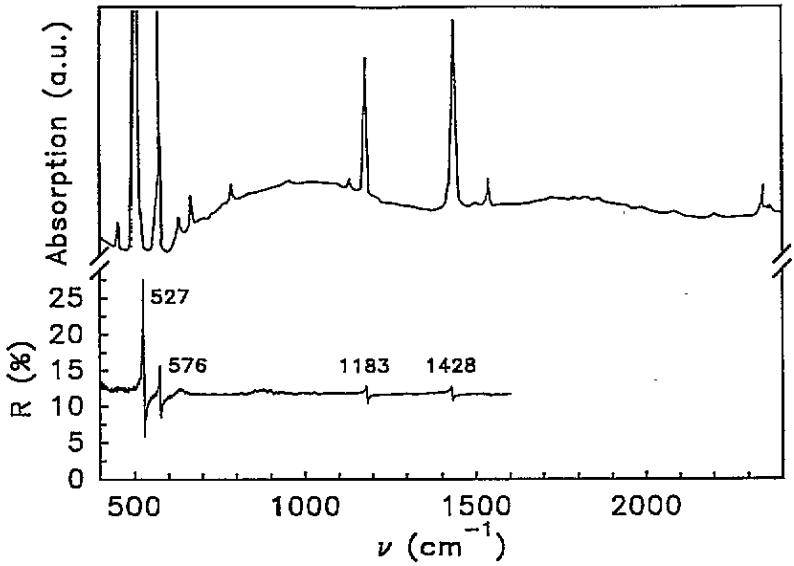

Figure 1. Infrared absorption for a thin film of C_{60} on Si after Krätschmer *et al* [2] (upper spectrum) and reflectivity for a single crystal from a {100} crystal face after Winkler *et al* [42] (lower spectrum). The numbers assigned to the structures in the reflectivity spectrum give the frequencies for the four IR allowed vibrational modes.

4.1. Fine structure of IR spectra

As can be seen there is a lot of fine structure in the spectra of figure 1. A blow-up of this structure was first reported by Chase *et al* [39] and interpreted as contributions from an IR response of I_h forbidden modes or overtones and combination tones. Similar results were observed later by Wang *et al* [40], Bowmar *et al* [41], and Martin et al. [23] for thin C_{60} films and by Winkler *et al* for single-crystal platelets [42]. As an example figure 2 shows a reflection spectrum for a thin single crystal with parallel {111} faces. The spectrum is

dominated by a very large number of lines from I_h forbidden modes (or overtones) which appear as a consequence of an absorption process due to the reflection at the rear side of the crystal. The size of these features is of the same magnitude as the structures in the reflectivity from the front surface for the IR allowed F_{1u} modes [42].

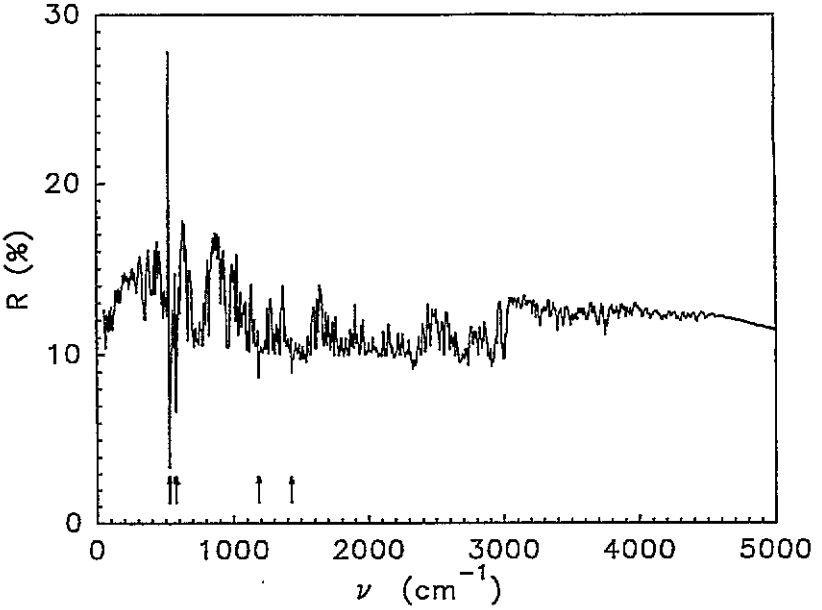

Figure 2. Infrared reflectivity of a 1 mm thick single-crystal platelet of C_{60} for the spectral range of the fundamental vibrational modes and overtones up to the third order. Arrows point to the fundamental F_{1u} modes; after Winkler *et al* [42].

Several authors have tried to correlate the individual peaks in such spectra to the 46 allowed vibrational modes in the molecule, including some overtones and difference frequencies. To do this a comparison with calculated line positions is necessary. This work is certainly cumbersome and the assignment is far from being unique but on the other hand this and similar results from Raman scattering turn out to be the only way to have experimental access to all vibrational modes. Since quantum chemical *ab initio* calculations are very reliable today it is worth having a look at listed frequencies obtained in this way. Table 2 gives a compilation of such results. The experimental data from IR spectroscopy are compared to calculations from a quantum chemical force field (QCFF/PI level) by Negri *et al* [43].

It is certainly important to know whether the additional modes observed appear as a consequence of the crystal field or from an isotope effect. Information on this problem was recently obtained from an analysis of spectra for isotope-enriched samples [44]. From a lack of any influence of the isotope concentration on the spectra the crystal field rather than the isotope effect was considered to be responsible for the relaxation of the selection rules.

4.2. High-resolution spectra and isotope effects

Recently vibrational IR spectra were recorded with very high resolution up to 0.014 cm^{-1} at low temperatures [45, 46]. Such experiments revealed intrinsic line widths as low as 0.5 cm^{-1} at these temperatures and a detailed splitting for all I_h allowed modes. Figure 3(*a*)

Table 2. Fundamental vibrational modes for the C_{60} molecule as observed from IR spectroscopy after Wang *et al* [40] and as calculated by Negri *et al* [43].

gerade modes			*ungerade* modes		
Species	IR	Theory	Species	IR	Theory
$A_{1g}(1)$	498	513	$A_{1u}(1)$	1143	1206
$A_{1g}(2)$	1470	1442			
$F_{1g}(1)$	502	597	$F_{1u}(1)$	527	544
$F_{1g}(2)$	976	975	$F_{1u}(2)$	579	637
$F_{1g}(3)$	1328	1398	$F_{1u}(3)$	1183	1212
			$F_{1u}(4)$	1429	1437
$F_{2g}(1)$	667	637	$F_{2u}(1)$	356	350
$F_{2g}(2)$	865	834	$F_{2u}(2)$	680	690
$F_{2g}(3)$	914	890	$F_{2u}(3)$	1026	999
$F_{2g}(4)$	1360	1470	$F_{2u}(4)$	1201	1241
			$F_{2u}(5)$	1577	1558
$G_g(1)$	486	476	$G_u(1)$	400	358
$G_g(2)$	621	614	$G_u(2)$	760	816
$G_g(3)$	806	770	$G_u(3)$	924	832
$G_g(4)$	1076	1158	$G_u(4)$	970	1007
$G_g(5)$	1356	1450	$G_u(5)$	1310	1401
$G_g(6)$	1525	1585	$G_u(6)$	1446	1546
$H_g(1)$	273	258	$H_u(1)$	343	403
$H_g(2)$	433	440	$H_u(2)$	563	531
$H_g(3)$	711	691	$H_u(3)$	696	724
$H_g(4)$	775	801	$H_u(4)$	801	812
$H_g(5)$	1101	1154	$H_u(5)$	1117	1269
$H_g(6)$	1251	1265			
$H_g(7)$	1427	1465			
$H_g(8)$	1578	11644			

shows as an example line shapes as obtained from single crystals at 10 K with a resolution of 0.014 cm^{-1}. As can be seen up to four lines appear which means the splitting is beyond the crystal field effect. It obviously results from an isotope contamination. This was confirmed by an investigation of isotope pure C_{60} as shown in figure 3(*b*) for $^{12}C_{60}$ and $^{13}C_{60}$ [47].

4.3. Temperature dependence of vibrational modes and phase transitions

Since the intrinsic line width for the vibrational modes is so small at low temperatures and rather broad at high temperatures the response of the line parameters to the temperature is important. Early work on this problem reported for thin films showed a strong increase of the line width for the F_{1u} modes starting at 200 K [48] but no discontinuity at the first-order phase transition. On the other hand Kamaras *et al* found a discontinuous appearance of new lines just below the phase transition [49]. The detailed behaviour of the fundamental IR-active lines was reported recently by Winkler *et al* [42] from single-crystal experiments. Nearly all line parameters were observed to change spontaneously at the temperature of the ordering transition. Figure 4 shows a series of reflectivity spectra in the spectral range of two selected F_{1u} modes. Spontaneous splitting at the order transition is well observed. It

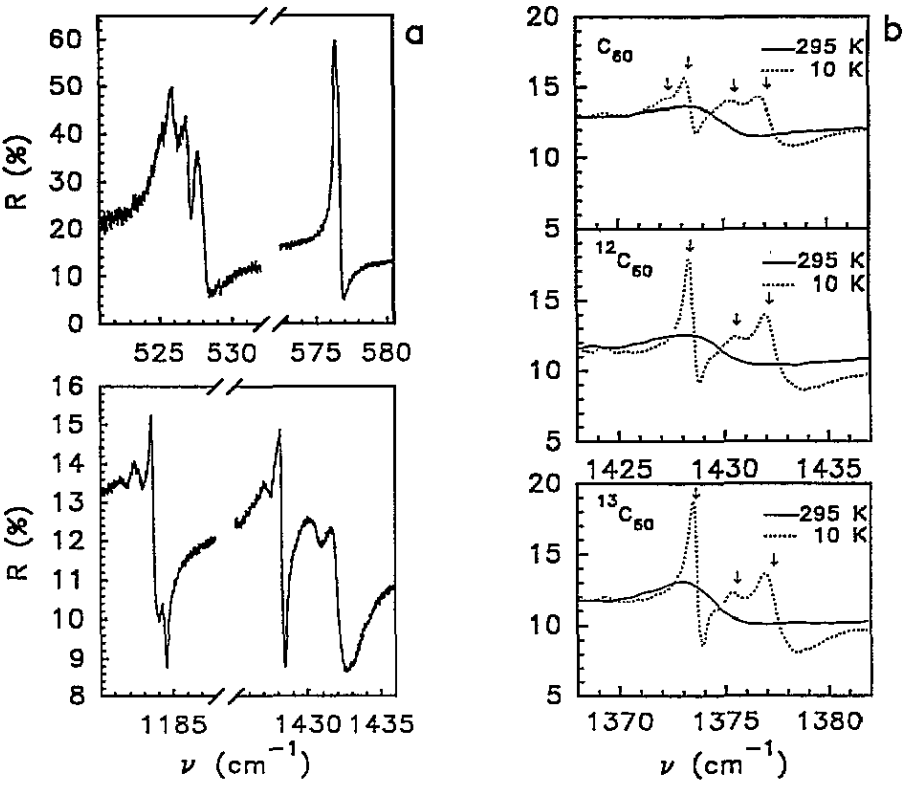

Figure 3. High-resolution IR reflectivity for the four fundamental modes at 10 K (a), after Winkler *et al* [46], and influence of the isotope mass on the spectra for one selected mode (b), after Homes *et al* [47]. Arrows in (b) indicate the line positions from a fit with harmonic oscillators.

cannot, however, be excluded that this splitting originates from a spontaneous narrowing of the line and is as such already present even at high temperatures. Support for this interpretation comes from an explicit plot of line width parameters which show indeed a spontaneous narrowing at 255 K as demonstrated for two F_{1u} modes in figure 4(*b*) and (*d*). The discontinuity in the line width may be not intrinsic for the high-frequency F_{1u} mode since we know from the description above that the line consists of several components. This difficulty is not effective for the F_{1u} mode at 577 cm^{-1} since here the splitting is only 0.1 cm^{-1} and thus much smaller than the line width at the transition temperature. Therefore the temperature dependence of the width for this line is of particular interest. It turns out that a simple three-phonon process (decay of the mode in two others with corresponding smaller energy) is not consistent with the experiment. This is demonstrated in figure 5 where the dashed line is representative of this process. The dramatic change of the line width and its strong increase with temperature suggests on the other hand that a coupling to the paralibrations is important. Comparing the damping with an exponential law as a function of the temperature indeed yields very good agreement and an activation energy of 56 meV which is very close to the activation for the rotational diffusion of 40 $\pm$ 10 meV as determined from NMR [51] and neutron scattering [52]. This was suggested to be very strong evidence for a dominating contribution of the rotational diffusion to the lifetime of the internal modes [50].

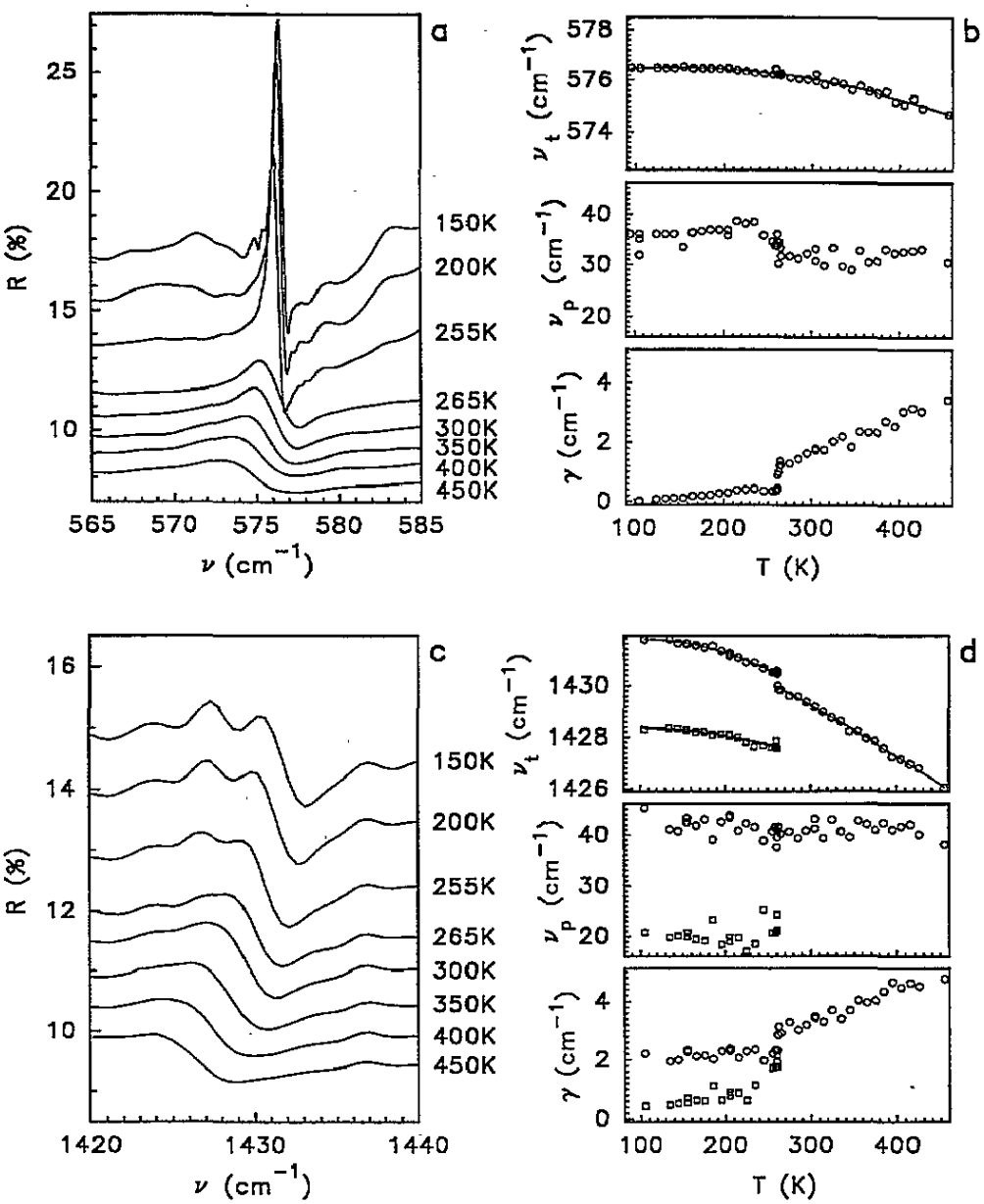

Figure 4. Reflectivity in the spectral range of the second-lowest- and of the highest-frequency F_{1u} mode for various temperatures as indicated (a), (c) and line parameters (position ν_t, oscillator strength ν_p^2 and width γ for the same modes (b), (d).

4.4. External modes

From table 1 we can expect two external modes for the low-temperature phase which should have a rather low energy, just above the librations. After some preliminary early work these modes were observed at 40 and 54 cm^{-1}, respectively [53, 54]. Figure 6 shows a transmission spectrum of a C_{60} crystallites taken at 10 K which in contrast to previous results

exhibits two clear structures at the frequencies mentioned above in very good agreement with results from inelastic neutron scattering [55].

5. IR spectroscopy of intercalated C_{60} with charge transfer

Infrared spectroscopy is widely used to study the intercalation process and the doped state of the fullerene salts. So far these experiments have been restricted to doping with alkali metals K, Rb, and Cs, however. Since nearly all alkali metal fullerenes are very air sensitive it is recommended to do the doping in a very inert atmosphere and check the response of the doping *in situ*.

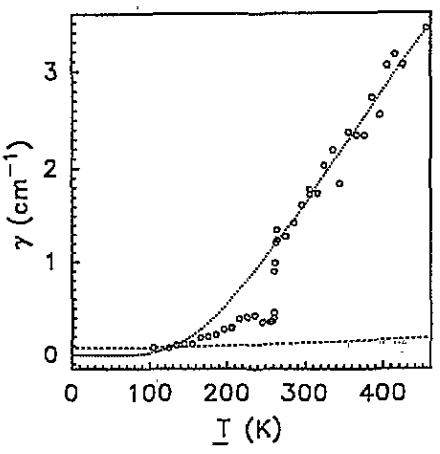

Figure 5. Line width versus temperature for the mode at 576 cm^{-1} (o) and behaviour according to a damping by a three-phonon process (– – –) and by coupling to rotational diffusion (·····), after [50].

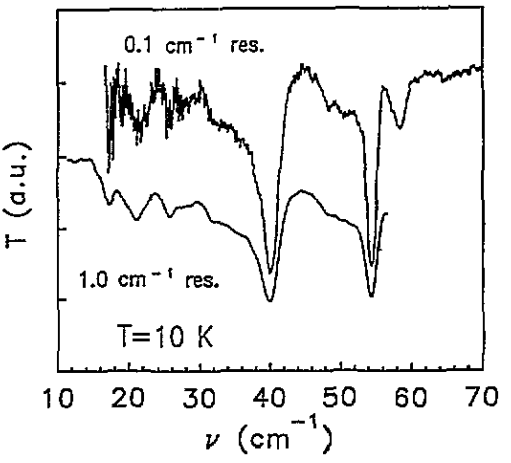

Figure 6. IR transmission from C_{60} crystallites at 10 K in the spectral range of the translational external modes, after *Horoyski and Thewalt [53]*. The top and the bottom curve are for 0.1 cm^{-1} and 1 cm^{-1} resolution, respectively.

5.1. Intercalating alkali metals in C_{60} fullerene

The salt state of the fullerenes can be reached by various processes. Originally the metal was diffused from the vapour phase into a thin film of the fullerene and the change of conductivity was detected *in situ*. Later doping of C_{60} powder was performed by heating stoichiometric quantities of the metal and of C_{60} in a sealed quartz tube at several hundred K and for several days. Occasionally alkali nitrides (AN_3) have been used for the doping process instead of the pure metal [56]. The alkali nitrides are stable at ambient conditions but decompose at the temperature where the doping process proceeds.

For the more bulky alkali metals K, Rb, and Cs four different doped states $(A^+)_xC_{60}^{x-}$ are known, as determined by the possible accommodation in the large interstitial lattice sites of the crystal. For $x = 1$ only the single octahedral site of the fcc lattice is occupied, for $x = 3$ the single octahedral and the two tetrahedral sites become occupied. For $x = 6$ a bcc lattice is established with six tetrahedral sites. $x = 4$ has a tetragonal crystal structure with distorted tetrahedral interstitial sites. Details of the crystal structures have been reviewed by

Table 3. Structures, lattice sites, and irreducible representations for IR-active vibrational modes for the various fullerides of K and Rb. Lattice constants are for K_nC_{60} at room temperature unless otherwise noted. Structures are represented by their reference space group.

n	Structure	Lattice constant (Å)	Lattice site for alkali	IR activity	
				Internal	External
0	T_h^3 $Fm\bar{3}$	$a = 14.17$ [57]		$22F_u$	
0	T_h^6 $Pa\bar{3}$ (LT)	$a = 14.04$ [60]		$87F_u$	$2F_u$
1	T_h^3 $Fm\bar{3}$	$a = 14,07$ [16]	octahedral $\times 1$	$22F_u$	
3	T_h^3 $Fm\bar{3}$	$a = 14.25$ [57]	octahedral $\times 1$ tetrahedral $\times 2$	$22F_u$	$2F_u$
4	D_{4h}^{17} $I/4mmm$	$a = 11.89$ [57] $c = 10.77$ [57]	tetrahedral $\times 4$ distorted	$F \rightarrow A + E$	
6	T_h^5 $Im\bar{3}$	$a = 11.39$ [57]	tetrahedral $\times 6$	$22F_u$	$3F_u$

Murphy *et al* [57], Fischer and Heiney [58], and Zhou and Cox [59]. The most important structural and symmetry properties for the alkali metal compounds are compiled in table 3.

Infrared activity is straightforwardly obtained from the point group in the structure and summarized in the second part of table 3. For the case of the external modes not only the vibrations of the molecules as for the pristine material but also those of the metal atoms contribute.

Only the structures with three alkali metals are metallic with respect to all of their physical properties. This is surprising and can be understood only from models which extend beyond a one-electron density functional approach. For the metallic phases contributions of the free carriers to the response function and possibly also the influence of electron pairing in the superconducting state is important.

The system AC_{60}, A = K, Rb, Cs was recently found to behave differently to the other structures. Their special properties will therefore be discussed in an extra section.

5.2. *Electronic spectra of thin films and single crystals*

The response from electronic transitions to the incident IR radiation was studied in several papers. It is of particular importance for the metallic systems A_3C_{60} but also for A_4C_{60}. Contributions from interband transitions, from transitions between subbands within the conduction band and from free carriers are considered. The response can be described in general by a phenomenological dielectric function of the form

$$\epsilon(\omega) = \epsilon_\infty + \epsilon_D(\omega) + \epsilon_{mir}(\omega) + \epsilon_T(\omega) \tag{2}$$

where ϵ_∞, ϵ_D, ϵ_{mir}, and ϵ_T account for the high-frequency contribution, the free-carrier contribution, a contribution from an oscillator in the mid-IR spectral range and a contribution from the t_{1u}–t_{1g} transition, respectively. Most experiments reported are for reflectivity from thin films obtained for the full spectral range. A subsequent Kramers–Kronig analysis allows us to study the optical conductivity or absorption and the full dielectric response function. For the Kramers–Kronig analysis the spectra from metallic samples are usually extrapolated to zero frequency by a Hagen–Rubens law. An example is given in figure 7. Part (a) shows the reflectivity for several different C_{60} compounds as measured over an energy range from 0.1 to 7 eV (400 cm^{-1} to 56 000 cm^{-1}). Part (b) presents the optical conductivity as obtained from a Kramers–Kronig transformation of the spectra. The sharp structures in the upper two

spectra of figure 7a originate from vibrations and will be discussed in the next paragraph. K_3C_{60} shows a Drude-like response in the low-frequency part whereas K_4C_{60} exhibits only a marginal increase of the reflectivity towards lower energy and Rb_6C_{60} remains flat. The structures in the high-energy part of the spectra are from interband transitions. They appear even more structured in the optical conductivity. Important information is contained in the very low-frequency limit of the spectra. Whereas for the metallic system the conductivity approaches a value of about 800 S cm^{-1} for zero frequency which is in reasonably good agreement with dc measurements, it becomes zero at about 800 cm^{-1} for K_4C_{60}, indicating that this compound is a semiconductor.

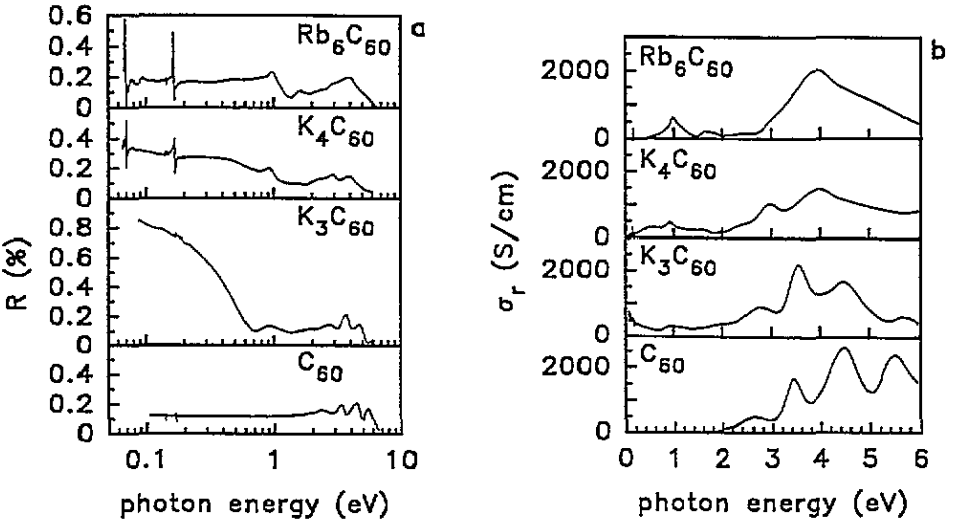

Figure 7. Reflectivity from C_{60} flakes for compounds indicated in the figure (a) and optical conductivity as obtained from a Kramers–Kronig analysis (b); after Iwasay and Kaneyasu [61].

A more quantitative interpretation of the FIR spectra is not straightforward. There is general agreement that the response is not simple Drude-like. In order to analyse the low-frequency part of the spectra shown above a response function of the form of equation 2 explicitly written as

$$\epsilon(\omega) = \epsilon_\infty + \omega_p^2 \left[-\frac{f_d}{\omega(\omega + i\gamma_p)} + \frac{1 - f_d}{\omega_{mir}^2 - \omega^2 + i\omega\gamma_{mir}} \right] + \frac{\omega_{pT}^2}{\omega_T^2 - \omega^2 - i\omega\gamma_T} \tag{3}$$

was used by Iwasay *et al.* In this equation ω_p and ω_{pT} are the plasma frequencies, ω_{mir} is the mid-IR oscillator frequency, ω_T the interband transition frequency and γ are the corresponding damping constants. f_d represents the relative fraction of the carriers contributing to the Drude response. A fit of this relation to the low-frequency part of the optical conductivity is shown in figure 8. The different behaviour for the metallic phases and for the semiconducting phases on approaching zero frequency as well as a contribution from a mid-IR band is evident. The mid-IR band around 0.4 to 0.5 eV may be considered as contributions from transitions within a split t_{1u} band. For the plasma frequency of the Drude component given as $\sqrt{f_d}\omega_p$ a value of 8640 cm^{-1} is obtained. This yields together with a free-carrier concentration of 4.1×10^{27} m^{-3} as evaluated from the size of the unit cell an effective free-carrier mass of 5 m_e in reasonably good agreement with calculations and other experimental results. From an interpretation of the mid-IR absorption as originating

from a pseudogap structure in the t_{1u} band Iwasay *et al* deduced a considerably smaller effective mass.

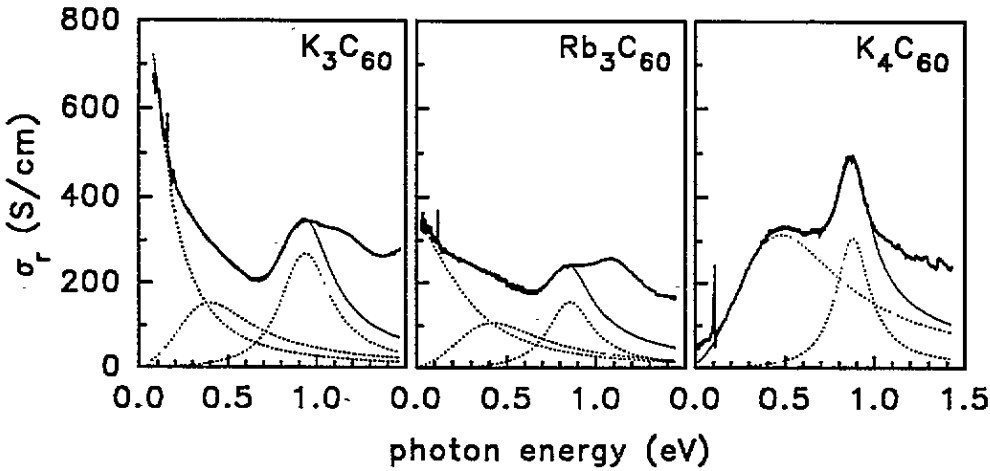

Figure 8. Optical conductivity for the low-frequency part of the reflectivity for the various phases A_xC_{60}. The dotted line represents the the fitted components according to equation 3; after Iwasay and Kaneyasu [61].

In several experiments by Degiorgi *et al* [27, 62] the reflectivity was measured to even lower frequencies and additional structure in the overall Drude response was observed. Using a similar relation to equation 3 the mid-IR oscillator was now assumed at much lower frequencies of the order of 500 cm^{-1}. From an overall oscillator strength as obtained by an integration over the FIR spectral range for K_3C_{60} (one-component model) a plasma frequency of 9491 cm^{-1} and consequently an effective band mass of 4 m_e was obtained in good agreement with the results of Iwasay *et al*. In a two-component picture where the Drude contribution and the mid-IR contribution were treated separately a three times lower plasma frequency resulted with a correspondingly more than ten times higher effective band mass. Interestingly as compared to the single-component picture this plasma frequency yields a London penetration depth which fits better to the results obtained from experiments in the superconducting state discussed below.

The origin of the various mid-IR oscillators is still under discussion. The model of a pseudogap as originally suggested by Takahashi *et al* [63] was not really confirmed later on which gives the interpretation of the 0.5 eV mid-IR absorption as an interband transition within the t_{1u} band more weight. If the low-energy mid-IR band around 500 cm^{-1} is really electronic and intrinsic its origin can not be derived from a simple one-electron picture.

5.3. Superconductivity

One of the most surprising results from the doped C_{60} compounds was their transition to superconductivity at rather high temperatures. It was certainly important in this connection to investigate the far-IR spectrum for a possible opening of a gap and to check the various types of phonon more carefully with respect to their activity in the pairing process. Several contributions to the first problem were reported by Degiorgi *et al* [62, 27, 64]. The reflectivity in the far IR was found to increase suddenly when the temperature was scanned through the transition to superconductivity at 19 K for K_3C_{60} and at 29 K for Rb_3C_{60}, finally reaching 100% for very low-temperatures. From a spectral analysis of the low temperature

reflectivity the onset of deviation from 100% was found around 50 and 60 cm^{-1} for the potassium and the rubidium compound, respectively. The exact values are best determined by a Kramers–Kronig transformation of the spectra and a subsequent analysis of the optical conductivity. As an example experimental results from Degiorgi *et al* [27] are shown in figure 9 for the rubidium compound. Similar spectra were obtained for potassium. As expected from BCS-like theories of superconductivity the real part of the optical conductivity becomes zero at the frequency which corresponds to the gap energy [65]. The results for the gap 2Δ obtained in this way were 48 and 60 cm^{-1} for the potassium and rubidium superconductor, respectively. Together with the corresponding transition temperatures this yields for the BCS ratio $2\Delta/k_BT_c$ the values 3.6 and 2.98 in good agreement with the classical result of 3.52 for weak-coupling superconductors. More recent experiments on single crystals gave values of 3.44 and 3.45 with even better agreement to the BCS result [64]. A check on the experimental results with a more sophisticated model based on the Eliashberg theory was found to be consistent with a pairing mechanism by high-frequency internal vibrations. The dominance of the high frequencies is, however, not generally agreed from other experiments.

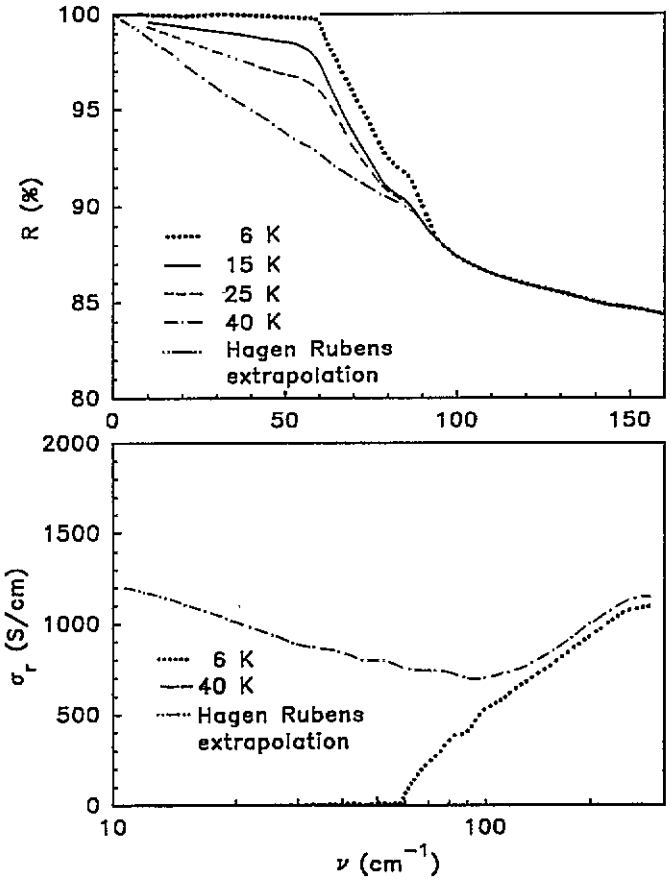

Figure 9. Far-IR reflectivity for Rb_3C_{60} at various temperatures above and below the transition to superconductivity (upper part), and real part of the optical conductivity as obtained from a Kramers–Kronig transformation (lower part); after Degiorgi *et al* [27].

In addition to information about the energy gap the penetration depth of the electromagnetic radiation can be evaluated from a comparison of the IR response in the normal and in the superconducting state. From the loss of spectral weight in the optical conductivity $\sigma(\omega)$ for the superconducting state the London depth λ can be evaluated as

$$\lambda^2 = c^2/8A \tag{4}$$

where A is the difference in the spectral weight of $\sigma(\omega)$ for the normal and for the superconducting state, respectively. In this way a penetration depth of 800 ± 50 nm was obtained for both K_3C_{60} and Rb_3C_{60} [27].

5.4. Vibrational spectra for charged C_{60}

Since the four F_{1u} modes are significant features for the undoped material their response to the intercalation was important and has been analysed in several papers [66, 22, 23]. As expected from previous work on the Raman lines and from the fact that antibonding states become occupied by the doping, at least three of the four modes undergo a downshift in frequency with increasing charge on the molecule. A detailed analysis was presented in [22]. Figure 10 shows the overall reflectivity of a thin film as grown for the various equilibrium phases. In the case of the monofulleride, Rb was used as a dopant since this compound was found to be more stable at room temperature as compared to the potassium compound. The wavelike response for $x = 0$ and $x = 6$ originates from thin-film interferences. Their absence in the spectra for $x = 1, 3$, and 4 is consistent with the metallic or narrow-gap nature of these materials as described above and in the next subsection. The sharp structures at the low-frequency end of the spectrum represent the F_{1u} modes. With the given background a line shape analysis was possible for these modes and the line shape parameters such as frequency, line width, and oscillator strength were evaluated for the different modes in all phases. The most important results can be summarized in a diagram and are shown in figure 11. The nearly linear downshift of the frequencies is consistent with a model developed by Rice and Choi in which the response of the vibrations to an interaction with the t_{1u} electrons is described [67]. In this 'charged phonon' model the coupling of the F_{1u} modes to virtual transitions of the electrons from t_{1u} to the next higher band which has t_{1g} symmetry was found to be the reason for the change in the IR response. The model also predicts a quadratic increase of the line intensities with the charge on the molecule which is well confirmed at least for the two modes shown in figure 11. For these charged phonon modes the electron–phonon coupling constants can be evaluated from a set of relations between the measured oscillator strengths $S(\omega_m) = (\pi\epsilon_0/2)\omega_{p,m}^2$ and the unrenormalized vibrational frequencies Ω_m where $\omega_{p,m}$ is the plasma frequency for the mth mode. These relations are evaluated as

$$S(\omega_m) = \frac{\pi N\alpha}{2} \Big/ \sum_n \lambda_n \frac{\Omega_n^2}{\Omega_n^2 - \omega_m^2} \tag{5}$$

where N is the number of C_{60} molecules per unit volume and α is the static electronic polarizability for the t_{1u}–t_{1g} transition. The evaluated dimensionless coupling constants λ_n for the two modes were found to be between 0.01 and 0.02.

From the simple group theoretical analysis given in section 3 the total symmetric A_g modes and the H_g modes are not IR active. However, they couple strongly to the t_{1u} electrons in the conduction band of the A_3C_{60} compounds and are presently considered to be responsible for the pairing process leading to superconductivity. This coupling can dress the *gerade* modes with a dipole moment and thus allows us to see them in an IR

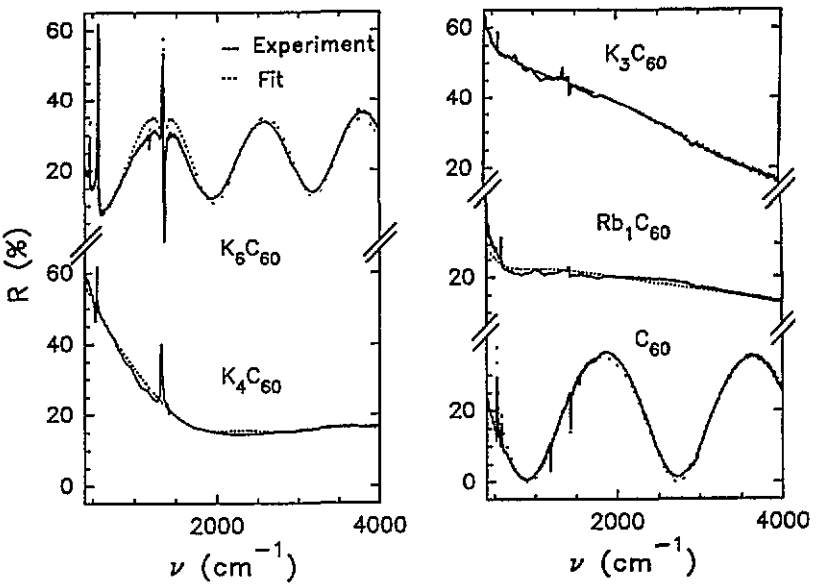

Figure 10. Overall response of a thin C_{60} film in the various phases A_xC_{60}, A = K, Rb, $x = 0, 1, 3, 4, 6$. The dotted line is as calculated for a multilayer response with a dielectric function similar to equation 3; after Pichler *et al* [22].

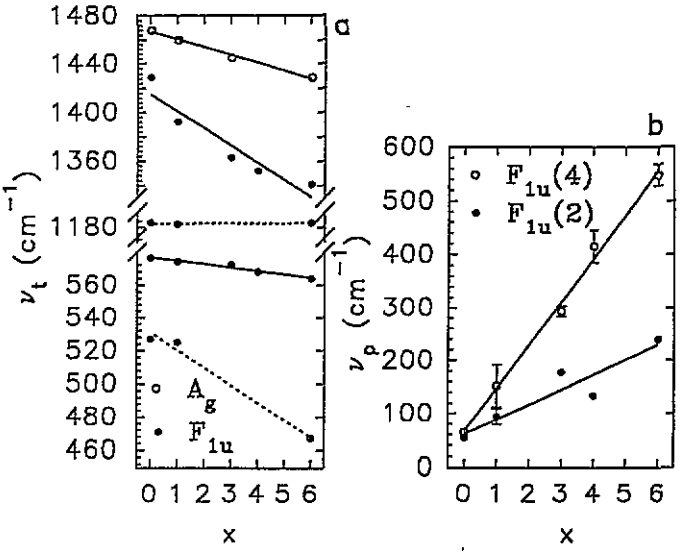

Figure 11. Line position ν_t and square root of oscillator strength ν_p versus charge x on the C_{60} molecule for the F_{1u} modes. In the case of the oscillator strength only results for modes observed in all five phases are given. The open circles refer to the shift for the Raman-active pinch mode for comparison; after Pichler *et al* [22].

spectrum. This behaviour is well known for organic charge transfer systems and conjugated polymers [68]. For the special symmetry of C_{60} some disorder turns out to be necessary to activate this process. Recent calculations showed that the intrinsic merohedral disorder in the A_3C_{60} compounds is big enough to trigger this effect [69, 70]. Structures in the IR

transmittance and reflectivity spectra of K_3C_{60} have been observed by Pichler *et al* [71] and were assigned to the *gerade* modes of A_g and H_g symmetry, respectively. From this results electron–phonon coupling constants in reasonably good agreement with calculated values could be evaluated. The assignment was straightforward particularly for the higher-frequency A_g mode (pinch mode).

6. Phase transitions and stability in systems with C_{60}^-

The phases with C_{60}^- have very special properties which will be discussed in this section. C_{60}^- has been obtained either from a doping process with alkali metals as described before or from a chemical reaction with a strong organic donor molecule like TDAE (tetrakis-diaethylaminoethylene). Interestingly the two types of compound behave oppositely with respect to stability under ambient conditions. Whereas TDAE C_{60} is extremely air sensitive RbC_{60} and probably also KC_{60} are stable in air, at least at room temperature as will be discussed in detail below.

6.1. The compounds AC_{60}

Alkali metal complexes AC_{60} were first observed by Raman scattering from thin films moderately doped with potassium at high temperatures [17]. These films showed a downshift of the most characteristic Raman line from 1469 cm^{-1} to 1463 cm^{-1} which is known to be characteristic for a change to a C_{60} monoanion. Cooling the film below a critical temperature resulted in a disproportionation of the system into undoped C_{60} and K_3C_{60}. These experiments were confirmed later by core level photoemission of the potassium atoms [18] and by Raman experiments from single crystals [72]. The crystal structure in the high-temperature phase was found to be rock salt [16] with the potassium ions at the octahedral interstitials. From line width measurements in NMR experiments the C_{60} ions were found to rotate with a moderate speed, much lower than that for the undoped material. Interestingly, the rubidium and the caesium compounds were observed to have the same high-temperature structure but exhibit a different dynamic on cooling. Instead of disproportionation they undergo a displacive phase transition of first order to an orthorhombic phase with possibly polymeric character as mentioned already. This polymeric character was claimed to be established by a 2 + 2 cycloaddition process along a face diagonal of the fcc lattice between two neighbouring C_{60} molecules. Support for this interpretation came from a detailed x-ray analysis from which an unusual short C_{60}–C_{60} distance of 0.91 nm in the direction of the cycloaddition ({110} of the original lattice) and an unusual extension of the carbon bonds on the molecules in the vicinity of the new bonds was found [73]. From a very recent analysis it was found that even for potassium a polymeric phase can be obtained if the samples are cooled with reasonable speed through the critical temperature of phase segregation [74, 75]. There is some evidence from electron spin resonance [76], NMR [77], and recently also from IR [75] that the orthorhombic state represents a quasi-one-dimensional metal. For rubidium and caesium this state is claimed to undergo a metal–insulator transition at 50 K to a spin-density wave state [76] whereas KC_{60} remains metallic to very low temperatures [75]. Finally, it was claimed that KC_{60} is stable to ambient conditions at room temperature [20]. This was proved recently from IR spectroscopy [78, 79] as will be demonstrated below.

Even though there are many open questions at present this system is obviously very multicoloured. As a general rule kinetic problems seem to play an important role for differences in the observed structural dynamics.

6.2. IR response for AC_{60}

IR spectroscopy for AC_{60} was first reported for thin films at room temperature as described above [22] but in these experiments no systematic study of the temperature dependence was performed and the signal to noise ratio in the spectra was too low to see the phase transition. In contrast recent measurements of the reflectivity from single crystals doped to RbC_{60} by the above described load and equilibrate technique gave a very clear response to the fcc to orthorhombic phase transition [78]. Figure 12 shows a series of reflectivity spectra taken at various temperatures from an {111} face of a single crystal which was doped to RbC_{60}. The first two parts of the figure are for the three lowest-frequency F_{1u} modes with a low resolution in temperature and the third is for the highest-frequency mode with a high resolution in temperature. From the figure it is evident that all four lines split into three components which is consistent with the low symmetry in the orthorhombic phase. Since the crystallographic point group for the new structure has D_{2h} symmetry the F_u species are correlated to the three IR-active modes with B_{1u}, B_{2u}, and B_{3u} character.

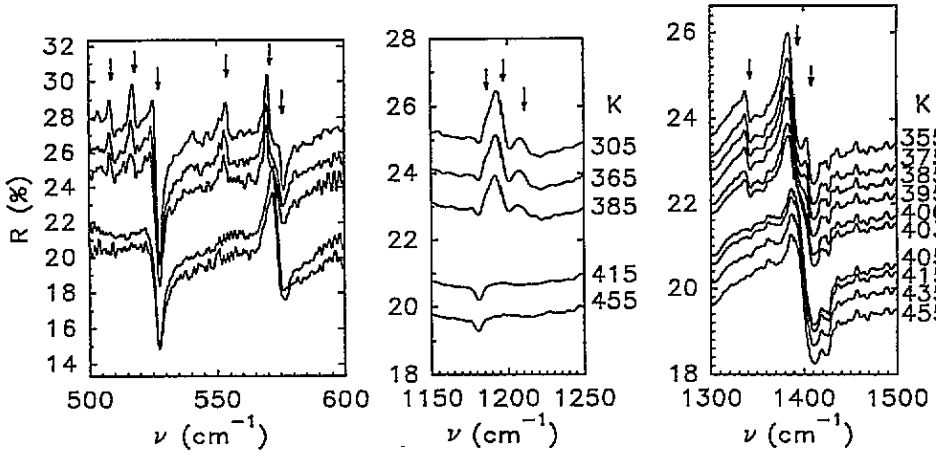

Figure 12. IR reflectivity from single-crystal RbC_{60} in the spectral range of the four fundamental F_{1u} modes for various temperatures. The values for the reflectivities are as measured. The arrows indicate the components of the F_{1u} mode in the orthorhombic phase.

From the details of figure 12 the phase transition occurs in a very narrow temperature range of a few degrees. This demonstrates its first-order character which was confirmed by a clear hysteresis between the cooling and heating cycle. With successive cycles through the transition T_c is downshifted and the transion broadens [80]. This indicates strong internal stresses accompanying the phase transition consistent with the very short C_{60}–C_{60} distances revealed from the x-ray analysis. Also, the very strong splitting observed for the $F_{1u}(4)$ mode in figure 12 is not consistent with a simple crystal field effect but rather indicates new covalent bonds.

The optical conductivity in the far-IR region is particularly instructive with respect to a possible metallic character of the orthorhombic phase. For KC_{60} this conductivity stays finite and even increases for a reduction of the frequency to zero. This means the conductivity behaves in a Drude-like way. For RbC_{60} the low-frequency conductivity starts to drop at a certain frequency and for a low enough temperature, indicating a transition to a state with a gap in the energy spectrum. This behaviour is demonstrated in figure 13 for the K and for the Rb compound, respectively.

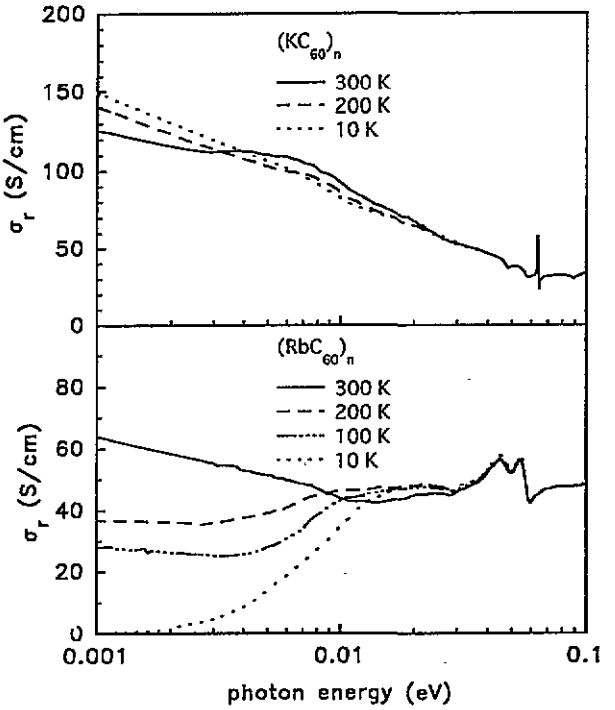

Figure 13. Spectral response of the optical conductivity for KC_{60} and RbC_{60} versus temperature; after Bommeli *et al* [75].

The air stability for RbC_{60} has been demonstrated recently very nicely from the IR reflectivity of a doped single crystal [78]. The crystal was doped to RbC_{60} and a spectrum in the full spectral range of the fundamental modes was recorded *in situ* in the cell. Then the cell was opened to air and the same type of spectrum was recorded during a full day. No change in the spectra was observed. An example of the recorded spectra is shown in figure 14. The original spectrum and the spectra recorded immediately after exposure to air and 24 hours after exposure to air are identical. This is proved in particular by the line at the bottom of the figure which represents the difference between the original recording and the spectrum after 24 hour exposure.

6.3. The system TDAE C_{60}

Except for the alkali and earth alkali metals at least one organic molecule was claimed to be a donor strong enough to reduce C_{60} to its monoanion by a charge transfer process in a crystal. The corresponding compound TDAE–C_{60}, where TDAE stands for tetrakis-dimethylaminoethylene, was found to undergo a 'soft' ferromagnetic or 'superparamagnetic' ordering transition at 16 K [81]. This transition is unusual in the sense that no spontaneous magnetization and no hysteresis can be observed. From ESR experiments unpaired spins (and charges) are claimed to be on the C_{60} molecule yielding a C_{60}^- ion which orders ferromagnetically below T_c. The corresponding other spin is claimed to be on the TDAE molecule and orders antiferromagnetically below T_c. Because of the large distance between the spins on the C_{60}^- ions the ferromagnetic coupling, if it exists, is very weak. Recent IR investigations on thin films and compressed pellets revealed several electronic interband

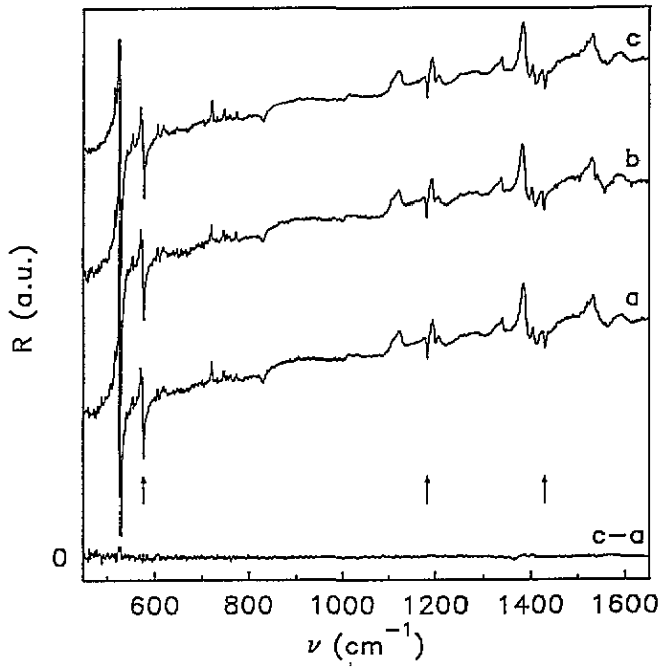

Figure 14. Single-crystal reflectivity of RbC_{60} as measured in vacuum (a), immediately after opening the cryostat (b), after 24 hours in air (c), and the difference between spectra (c) and (a); after Winkler *et al* [78].

transitions in the background of the spectra which may originate from the extra electron in the t_{1u} conduction band but a real metallic state could not be observed [82, 83]. In addition to that a considerable number of sharp lines occurs which originate from vibrations of the C_{60} and of the TDAE molecule. Figure 15 shows as an example the transmission from a TDAE–C_{60} film on a gold substrate. The broad background absorption represents the electronic interband transitions. From the sharp absorption lines those at 524 cm^{-1}, 572 cm^{-1}, 1185 cm^{-1}, and 1427 cm^{-1} were assigned to the four fundamental and symmetry-allowed F_{1u} modes of C_{60}. The surprising result is the lack of any charge-induced line shift if compared to e.g. the results of figure 11. This is in contrast to all observations from IR spectroscopy so far and not at all understood at present.

In this connection it is very interesting to note that for another organic compound with C_{60} a charge transfer to C_{60} was found in the IR spectra but no significant consequences with respect to conductivity or unusual magnetic properties appeared. This crystal was $(Ph_4P)C_{60}I$ where Kamaras *et al* observed a downshift of the highest-frequency F_{1u} mode to 1394 cm^{-1} which is, according to figure 11, in reasonable agreement with a single negatively charged C_{60} [84].

7. Higher fullerenes, endohedral fullerenes and carbon nanotubes

Only a few papers have reported on IR spectra from higher fullerenes and from endohedral fullerenes. As outlined at the beginning the simplest higher fullerene is C_{70} which has a single isolated pentagon isomer with D_{5h} symmetry. This symmetry allows only one- and two-dimensional representations for molecular wave functions. Accordingly, the 204

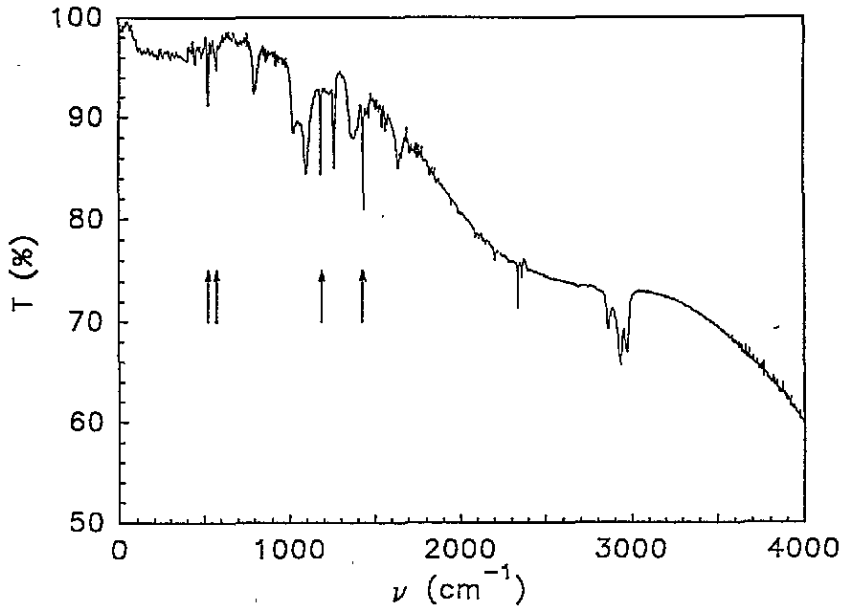

Figure 15. IR transmission from a thin film of TDAE–C_{60} on gold. The arrows indicate the positions for the four F_{1u} modes; after Bommeli *et al* [83].

vibrational degrees of freedom yield a total of 122 vibrational modes distributed as

$$\Gamma_{tot} = 10A_2'' + 21E_1' + 12A_1' + 22E_2' + 19E_1'' + 9A_2' + 9A_1'' + 20E_2'' \qquad (6)$$

from which only the A_2'' and the E_1' species are IR active. In a recent paper by Jishi *et al* [85] frequencies for all IR-active modes and for the 53 Raman-active modes were calculated and a reasonable number of them were observed experimentally. The IR spectrum is dominated by a strong line at 1431 cm^{-1} and several accumulated lines in the 500 to 700 cm^{-1} region. Similar experimental results were previously reported by Varma *et al* [86]. A temperature dependence for some of the internal modes of the C_{70} molecule was reported by Katayama *et al* [87].

Going to even larger molecules like e.g. C_{76} the symmetry is reduced further and the number of modes increases correspondingly. The most stable isomer in the latter molecule has D_2 symmetry which allows only one-dimensional representations and all species except the A modes are IR-active. This yields 165 IR active vibrations. A thin-film spectrum was reported recently by Michel *et al* [88]. It looks similar to that for C_{70} but the dominating line in the C=C stretch region is shifted to 1441 cm^{-1}. Obviously this line tends to shift eventually to the well known E_{1u} mode at 1587 cm^{-1} in highly oriented pyrolytic graphite with fully planar carbon sheets.

Before the final limit of planar carbon sheets is reached the carbon nanotubes scale. Recently published IR spectra indeed showed an intermediate frequency of 1575 cm^{-1} at least for the E_{1u} mode [89].

8. Fulleroides

IR spectroscopy has bee used repeatedly to characterize new molecules derived from the fullerenes. Examples are organodihydrofullerenes were a double bond is opened and one hydrogen and various alkanes are added. Since in this case the symmetry is strongly reduced

but otherwise the influence on the rest of the fullerene is not very strong the IR spectra show a splitting of the F_{1u}-derived modes and new background lines but overall the original spectrum from C_{60} is still recognizable [90]. Similar results were obtained for fluorinated C_{60} [91]. In contrast, the IR spectrum of C_{60} is completely changed for various degrees of bromination. The lower the degree of bromination the more complicated becomes the spectrum [92].

Acknowledgments

We acknowledge valuable discussions with J Winter and L Mihaly and the supply of the most recent IR spectra for isotope clean C_{60} by Professor Thewalt prior to publication. This work was supported by the Österreichische Nationalbank, project 4507.

References

[1] Kroto H, Heath J R, O'Brien S C, Curl R F and Smalley R E 1985 *Nature* **318** 162
[2] Krätschmer W, Lamb L D, Fostiropoulos K and Huffman D R 1990 *Nature* **347** 354
[3] Meng R L, Ramirez D, Jiang X, Chow P C, Diaz C, Matsuishi K, Moss S G, Hor P H and Chu C W 1991 *Appl. Phys. Lett.* **5** 3402
[4] Haluska M, Kuzmany H, Vybornov M, Rogl P and Fejdi P 1993 *Appl. Phys.* A **56** 161
[5] Cox D E, Fujii Y, Sawatzky G A and Shelton R N (ed) 1993 *J. Phys. Chem. Solids* **54** No 12
[6] Kuzmany H 1993 *Appl. Phys.* A **56** No 3
[7] 1994 *Solid State Physics* vol 48 (New York: Academic)
[8] Kuzmany H, Matus M, Burger B and Winter J 1994 *Adv. Mater.* **6** 731
[9] Heiney P A, Fischer J E, McGhie A R, Romanow W J, Denenstein A M, McCauley J P Jr and Smith A B III 1991 *Phys. Rev. Lett.* **66** 2911
[10] Gugenberger F, Heid R, Meingast C, Adelmann P, Braun M, Wühl H, Haluška M and Kuzmany H 1992 *Phys. Rev. Lett.* **69** 3774
[11] Schranz W, Fuith A, Dolinar P, Warhanek H, Haluška M and Kuzmany H 1993 *Phys. Rev. Lett.* **71** 1561
[12] van Tendeloo C, Amelinckx S, Verheijen M A, van Loosdrecht P M H and Meijer G 1992 *Phys. Rev. Lett.* **96** 7424
[13] Haddon R C, Hebard A F, Rosseinsky M J, Murphy D W, Duclos S J, Lyons K B, Miller B, Rosamilia J M, Fleming R M, Kortan A R, Glarum S H, Makhija A V, Muller A J, Eick R H, Zahurak S M, Tycko R, Dabbagh G and Thiel F A 1991 *Nature* **350** 320
[14] Hebard A F, Rosseinsky M J, Haddon R C, Murphy D W, Glarum S, Palstra T T M, Ramirez A P and Kortan A R 1991 *Nature* **350** 600
[15] Tanigaki K, Ebbesen T W, Saito S, Mizuki J, Tsai J S, Kubo Y and Kuroshi S 1991 *Nature* **352** 222
[16] Zhou Q, Zhou O, Bykovetz N, Fischer J E, MacGhie A R, Romanow W J, Lin C L, Strongin R M, Cichy M A and Smith A B III 1993 *Phys. Rev.* B **47** 13948
[17] Winter J and Kuzmany H 1992 *Solid State Commun.* **84** 935
[18] Poirier D M and Weaver J H 1993 *Phys. Rev.* B **47** 10959
[19] Pekker S, Forro L, Mihaly L and Janossy A 1994 *Solid State Commun.* **90** 349
[20] Pekker S, Janossy A, Mihaly L, Chauvet O, Carrard M and Forro L 1994 *Science* **265** 1077
[21] Pichler T, Kürti J and Kuzmany H 1993 *Condens. Matter Mater. Commun.* **1** 21
[22] Pichler T, Winkler R and Kuzmany H 1994 *Phys. Rev.* B **49** 15879
[23] Martin M C, Du X, Kwon J and Mihaly L 1994 *Phys. Rev.* B **50** 173
[24] Iwasa K, Tanaka K, Yasuda T and Koda T 1992 *Phys. Rev. Lett.* **69** 2284
[25] Rotter L D, Slesinger Z, McCauley J P Jr, Coustel N, Fischer J E and Smith A B III 1992 *Nature* **355** 532
[26] Fitzgerald S A, Kaplan S C, Rosenberg A, Sievers A J and McMordies R A S 1992 *Phys. Rev* **45** 10165
[27] Degiorgi L, Nicol E J, Klein O, Grüner G, Wachter P, Huang S M, Wiley J and Karner R B 1994 *Phys. Rev.* B **49** 7012
[28] Achiba Y, Kikuchi K, Wakabayashi T, Nakahara N and Suzuki S 1992 *Advanced Series in Fullerenes* vol 2, ed C Taliani, G Ruani and R Zamboni (Singapore: World Scientific) p 13
[29] Michel R H, Kappes M M, Adelmann P and Roth G 1994 *Angew. Chem.* **106** 1742

[30] Michel R H, Fuchs D, Beck R D and Kappes M M 1995 *Proc. Int. Winter School on Electronic Properties of Novel Materials (Kirchberg, 1995)* (Singapore: World Scientific) at press
[31] Poirier D M, Knupfer M, Weaver J H, Andreoni W, Laasonen K, Parinello M, Bethune D S, Kikuchi K and Achiba Y 1994 *Phys. Rev.* B **49** 17 403
[32] Andreoni W and Curioni A 1994 *Proc. Int. Winter School on Electronic Properties of Novel Materials (Kirchberg, 1994)* ed H Kuzmany, J Fink, M Mehring and S Roth (Singapore: World Scientific) p 93
[33] Taylor R and Walton D R M 1993 *Nature* **363** 685
[34] Hirsch H, Lamparth I, Grösser T, Prato M, Lucchini V and Wudl F 1995 *Proc. Int. Winter School on Electronic Properties of Novel Materials* (Singapore: World Scientific) at press
[35] Dresselhaus G, Dresselhaus M S and Eklund P C 1992 *Phys. Rev.* B **45** 6923
[36] Tanaka Y, Tokumoto M and Sugawa Y 1995 *Fullerene Sci. Technol.* **3** 179
[37] Weeks D E 1992 *J. Chem. Phys.* **96** 7380
[38] Wu Z C, Jelski D A and George T J 1987 *Chem. Phys. Lett.* **137** 291
[39] Chase B, Herron N and Holler E 1992 *J. Chem. Phys.* **96** 4262
[40] Wang K A, Rao A M, Eklund P C, Dresselhaus M S and Dresselhaus G 1993 *Phys. Rev.* B **48** 11 375
[41] Bowmar P, Kurmoo K, Green M A, Pratt F L, Hayes W, Day P and Kikuchi K 1993 *J. Phys.: Condens. Matter* **5** 2739
[42] Winkler R, Pichler T and Kuzmany H 1994 *Z. Phys.* **96** 39
[43] Negri F, Orlandi G and Zerbetto F 1988 *Chem. Phys. Lett.* **144** 31
[44] Martin M C, Fabian J, Godard J, Bernier P, Lambert J M and Mihaly L 1995 *Phys. Rev.* B **51** 2844
[45] Homes C C, Horoyski P J, Thewalt M L W and Clayman B P 1994 *Phys. Rev.* B **49** 7052
[46] Winkler R, Kuzmany H and Keens A unpublished
[47] Homes C C, Horoyski P J, Thewalt M L W, Clayman B P and Anthony T R 1995 *Phys. Rev.* B at press
[48] Narasimhan L R, Stonebeck D N, Hebard A F and Patel C K N 1992 *Phys. Rev.* B **46** 2591
[49] Kamaras K, Akselrod L, Roth S, Mittelbach A, Hönle W and von Schnering H G 1993 *Chem. Phys. Lett.* **214** 338
[50] Winkler R 1994 *Diplomarbeit* University of Vienna
[51] Johnson R D, Yannoni C S, Dorn H, Salem J R and Bethune D S 1992 *Science* **255** 1235
[52] Neumann D A *et al* 1991 *Phys. Rev. Lett.* **67** 3808
[53] Horoyski P J and Thewalt M L W 1993 *Phys. Rev.* B **48** 11 446
[54] Agladze N I, Zhizhin G N, Klimin S A, Haluska M and Kuzmany H 1994 *Opt. Spectrosc.* **76** 241
[55] Pintschovius L, Renker B, Gompf F, Heid R, Chapot S L, Haluska M and Kuzmany H 1992 *Phys. Rev. Lett.* **69** 2662
[56] Tokumoto M, Tanaka Y, Kinoshita N, Kinoshita T, Ishibashi S and Ikara H 1993 *J. Phys. Chem. Solids* **54** 1667
[57] Murphy D M, Rosseinsky M J, Fleming R M, Tycko R, Ramirez A P, Haddon R C, Siegrist T, Dabbagh G, Tully J C and Walstedt R E 1992 *J. Phys. Chem. Solids* **53** 1321
[58] Fischer J E and Heiney P A 1993 *J. Phys. Chem. Solids* **54** 1725
[59] Zhou O and Cox D E 1992 *J. Phys. Chem. Solids* **53** 1373
[60] David W I F, Ibberson R M, Dennis T J S, Hare J P and Prassides K 1992 *Europhys. Lett.* **18** 219
[61] Iwasay Y and Kaneyasu T 1995 *Phys. Rev.* B **51** 3678
[62] Degiorgi L, Wachter P, Grüner G, Huang S M, Wiley J and Kaner R B 1992 *Phys. Rev. Lett.* **68** 2987
[63] Takahashi T, Suzuki S, Morikawa T, Katayama-Yoshida H, Asegawa S H, Inokuchi H, Seki K, Kikuchi K, Suzuki S, Ikemoto K and Achiba Y 1992 *Phys. Rev. Lett.* **68** 1232
[64] Degiorgi L, Briceno G, Fuhrer M S, Zettl A and Wachter P 1994 *Nature* **368** 541
[65] Mattis D C and Bardeen J 1958 *Phys. Rev.* **111** 412
[66] Fu K J, Karney W L, Chapman O L, Huang S M, Kamer R B, Diederich F, Holzer K and Wetten R 1992 *Phys. Rev.* B **46** 1937
[67] Rice M J and Choi H Y 1992 *Phys. Rev.* B **45** 10 173
[68] Rice M J, Pietronero L and Brüsch P 1977 *Solid State Commun.* **21** 757
[69] Deshpande M S, Mele E J, Rice M J and Choi H Y 1994 *Phys. Rev.* B **50** 6993
[70] Deshpande M S, Mele E J, Rice M J and Choi H Y 1995 *Phys. Rev.* B at press
[71] Pichler T, Matus M and Kuzmany H 1993 *Solid State Commun.* **86** 221
[72] Winter J and Kuzmany H 1993 *Proc. Int. Winter School on Electronic Properties of Novel Materials (Kirchberg, 1993) (Springer Series in Solid-State Sciences 117)* ed H Kuzmany *et al* (Berlin: Springer) p 81
[73] Stephens P, Bortel G, Faigel G, Tegze M, Janossy A, Pekker S, Oszlanyi G and Forro L 1994 *Nature* **370** 636

[74] Winter J and Kuzmany H 1995 *Phys. Rev.* B at press
[75] Bommeli F, Degiorgi L, Wachter P, Legeza Ö, Janossy A, Oszlanyi G, Chauvet O and Forro L 1995 *Phys. Rev.* B **51** 14794
[76] Chauvet O, Oszlanyi G, Forro L, Stephens P W, Tegze M, Faigel G and Janossy A 1994 *Phys. Rev. Lett.* **72** 2721
[77] Tycko R, Dabbagh G, Murphy D W, Zhu Q and Fischer J E 1993 *Phys. Rev.* B **48** 9097
[78] Winkler R, Pichler T and Kuzmany H 1995 *Appl. Phys. Lett.* **66** 1211
[79] Martin M C and Mihaly L 1995 *Appl. Phys. Lett.* **66** 1015
[80] Pichler T unpublished.
[81] Allemand P M, Khemani K C, Koch A, Wudl F, Holczer K, Donavan S, Grüner G and Thomson J D 1991 *Science* **253** 301
[82] Mihailovic D, Venturini P, Hassanian A, Gasperic J, Lutar K and Milicev S 1994 *Proc. Int. Winter School on Electronic Properties of Novel Materials 'Progress in Fullerene Research' (Kirchberg, 1994)* ed H Kuzmany *et al* (Singapore: World Scientific) p 275
[83] Bommeli F, Degiorgi L, Wachter P, Mihailovic D, Hassanian A, Venturini P, Schreiber M and Diederich F 1995 *Phys. Rev.* B **51** 1366
[84] Kamaras K, Katsumoto K, Wojnowski M, E. Schönherr, Klos H and Gotschy B 1994 *Proc. Int. Winter School on Electronic Properties of Novel Materials 'Progress in Fullerene Research'* ed H Kuzmany *et al* (Singapore: World Scientific) p 357
[85] Jishi R A, Dresselhaus M S, Dresselhaus G, Wang K A, Zhou P, Rao A M and Eklund P 1993 *Chem. Phys. Lett.* **206** 187
[86] Varma V, Seshardi R, Govindaraj A, Sood A K and Rao C N R 1993 *Chem. Phys. Lett.* **203** 545
[87] Katayama N, Miyatake Y, Okazaki Y, K. Kikuchi, Achiba Y, Kiemoto I and Iriyama K 1993 *Fullerene Sci. Technol.* **1** 329
[88] Michel R H, Schreiber H, Gierden R, Hennrich F, Rockenberger J, Beck R D and Kappes M M 1994 *Ber. Bunsenges. Phys. Chem.* **98** 975
[89] Kastner J, Pichler T, Kuzmany H, Curran S, Blau W, Weldon D N, Delamesiere M, Draper S and Zandbergen H 1994 *Chem. Phys. Lett.* **221** 53
[90] Hirsch H, Grösser T, Skiebe A and Soi A 1993 *Chem. Ber.* **126** 1061
[91] Hamwi A, Fabre C, Chaurand P, Della-Negra S, Ciot C, Djurado D, Dupuis J and Rassat A 1993 *Fullerene Sci. Technol.* **1** 499
[92] Birkett P R, Hitchcock P B, Kroto H W, Taylor R and Walton D R M 1992 *Nature* **357** 479